Thermochimica Acta, 189 (1991) 129–141
Elsevier Science Publishers B.V., Amsterdam

Phase equilibria in the Fe_2O_3–V_2O_5–MoO_3 system

Maria Kurzawa

Institute of Fundamental Chemistry, Technical University of Szczecin, Al. Piastów 42, 71-065 Szczecin (Poland)

(Received 31 January 1991)

Abstract

The phase equilibria established in the Fe_2O_3–V_2O_5–MoO_3 system over the whole component concentration range to 1000 °C have been studied by DTA and X-ray powder diffraction methods. The experimental results are presented graphically in the form of projections of the solidus and liquidus planes of the Fe_2O_3–V_2O_5–MoO_3 system on the plane of the component concentration triangle. Isothermal cross-sections of the phase equilibria diagram, and sections in which the contents of one of the oxides are constant have also been constructed.

INTRODUCTION

A literature survey has shown that both the oxides Fe_2O_3, V_2O_5 and MoO_3, and the phases that exist in the two-component systems comprising the Fe_2O_3–V_2O_5–MoO_3 system, exhibit interesting catalytic properties [1–3]. Vanadium(V) oxide has been known for years as a catalyst for the oxidation of SO_2 to SO_3, and for the sulfonation and oxidation of aromatic hydrocarbons [3]. Like MoO_3, it is also a fundamental component of the catalysts used for the oxidation of benzene to maleic anhydride [4]. In addition, mixtures of MoO3 and $Fe_2(MoO_4)_3$, the sole compound existing in the Fe_2O_3–MoO_3 system, are used in industry as catalysts for the oxidation of methanol to formaldehyde [5]. It is known that the addition of other oxides, e.g. Fe_2O_3, may influence the activity, selectivity and useful life of a catalyst [4,6].

The study of the mechanism of a catalytic process involving a solid catalyst requires a thorough and comprehensive knowledge of the solid body on the surface of which the elementary catalytic event occurs. This knowledge is achieved by the study of the nature and compositions of the phases occurring in a system typical of the catalyst, and by investigating the structure and properties of the phases as well as those of the phase equilibria being established in the system of interest; the equilibria supply information on the stability of the phases existing in that system. Therefore, it seemed

0040-6031/91/$03.50

relevant to investigate the phase equilibria in the three-component system of some transition metal oxides, that is, Fe_2O_3–V_2O_5–MoO_3.

The basic properties and the structure, both of the components of interest and of some of the phases existing in the two-component systems, Fe_2O_3–MoO_3, Fe_2O_3–V_2O_5 and V_2O_5–MoO_3, are well known [7–13]. The phase equilibrium diagrams of the two-component systems are also well known [7,9,11]. On the other hand, investigations of the three-component system Fe_2O_3–V_2O_5–MoO_3 have been reported only by Walczak and co-workers [14–22]. Their work has shown that the components of the system form two compounds, $FeVMoO_7$ and $Fe_4V_2Mo_3O_{20}$, which melt incongruently [14,15]

$$FeVMoO_7(s) \overset{680\pm5\,^\circ C}{\rightleftarrows} Fe_4V_2Mo_3O_{20}(s) + \text{liquid} \quad (1)$$

$$Fe_4V_2Mo_3O_{20}(s) \overset{760\pm5\,^\circ C}{\rightleftarrows} Fe_2(MoO_4)_3(s) + Fe_2O_3(s) + \text{liquid} \quad (2)$$

It has also been established that a substitution solid-solution of MoO_3 in $Fe_2V_4O_{13}$, a compound existing in the Fe_2O_3–V_2O_5 system, in which the V^{5+} ions are substituted by Mo^{6+} in the lattice of the solution matrix, takes place in the system. Compensation of the excessive positive charge results from the reduction of an equivalent amount of Fe^{3+} to Fe^{2+} [16]. The solubility limit of MoO_3 in $Fe_2V_4O_{13}$ at ambient temperature is about 18 mol.% of MoO_3, whereas at the solidus line temperature it is about 20 mol.% of MoO_3, in the starting mixture of oxides [17,18]. The research of Walczak and co-workers has determined that phase equilibria are established only in selected pseudo-two-component systems—sections of the three-component system [19–22]. On the other hand, the diagram for the phase equilibria of the Fe_2O_3–V_2O_5–MoO_3 system has yet to be established. The aim of this study was to determine the nature of the phases coexisting at equilibrium in the three-component system, both in the solid state and above the solid line, over the whole component concentration range to 1000 °C.

Two short communications on these investigations have been presented at conferences [23,24].

EXPERIMENTAL

The starting materials, of reagent grade (POCh), were V_2O_5, Fe_2O_3 and MoO_3 (obtained by thermal decomposition of $(NH_4)_6Mo_7O_{24} \cdot 4\,H_2O$ at 150—450 °C in air). The other separately obtained compounds were $Fe_2(MoO_4)_3$, $FeVO_4$, $V_9Mo_6O_{40}$, $FeVMoO_7$, $Fe_4V_2Mo_3O_{20}$, a solid solution of MoO_3 in $Fe_2V_4O_{13}$ with 20 mol.% MoO_3 and a solid solution of MoO_3 in V_2O_5 with 30 mol.% MoO_3. The $V_9Mo_6O_{40}$ phase was obtained by the precipitation method described by Jarman and Cheetham [12] and Jarman et al. [25]; the other phases were obtained by the reaction in the solid state between appropriate mixtures of the oxides Fe_2O_3, V_2O_5 and MoO_3, under conditions described in the literature [7,9,11,14,15]. X-ray powder diffraction

has shown that all the preparations consist of a single phase. The DTA curves of these preparations record only their melting.

DTA studies were made on a Paulik–Paulik–Erdey derivatograph, using quartz crucibles, in air, at 20–1000 °C with a heating rate of 10 °C min^{-1}. The weight of each sample examined was 1000 mg. In order to construct a phase diagram, solidus lines and planes were determined based on the temperature at which the DTA effect begins, whereas the liquidus curves were based on the temperature at which the effect peaks. The temperature-reading accuracy, based on repetitions, was found to be ±5 °C.

The phase composition of the preparations was established by X-ray powder diffraction (diffractometer DRON-3, Co $K\alpha$) referring to data in the PDF cards [26] and in the literature [9,12,14,15].

A basic series of preparations containing 36 samples was made from oxides. The content of one of the oxides in the preparations was constant, whereas those of the other two components varied in steps of 10%. An additional series of 14 samples was prepared, from areas and sections that required supplementary investigations. The oxides, weighed in appropriate proportions, were mixed by grinding, pastilled and heated under conditions

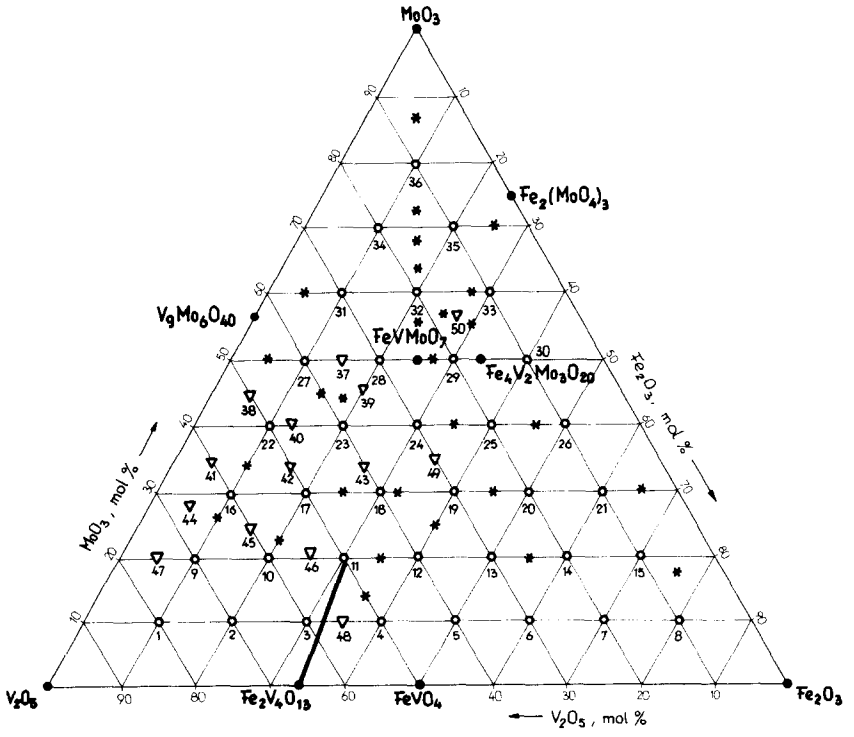

Fig. 1. Position of the basic series samples (○), additional samples (▽) and of verification samples (*).

that led to the equilibrium state, i.e.

400 °C → 500 °C (1 h); 500 °C (24 h); 550 °C (24 h); 550 °C (72 h).

The samples of the basic series were cooled slowly to ambient temperature, but the samples from the additional series continued to be heated at 570 °C over 72 h and were then cooled rapidly to ambient temperature. The samples of both series were ground, examined by DTA, and their phase composition was than established. In this way, it was possible to establish the kinds of phases formed and their coexistence ranges in the subsolidus area. The positions of the samples of both series in the field of the composition concentration triangle of the Fe_2O_3–V_2O_5–MoO_3 system are shown in Fig. 1.

Irrespective of this, some physical mixtures of the phases were prepared for a final verification of the subsolidus area, the phases being considered, on the grounds of experimental results with preparations from the basic and additional series, as equivalent in particular fields and sections of the subsolidus area. The compositions of these mixtures are also marked in Fig. 1.

The mixtures were heated for 72 h at temperatures 20 °C lower than those of the appropriate solidus planes or lines; they were then cooled rapidly to ambient temperature, ground and their phase compositions were then investigated.

RESULTS AND DISCUSSION

Table 1 shows the X-ray powder diffraction results for preparations in the equilibrium state, obtained for both the basic and the additional series. The results from the phase analysis indicate that oxides, the components of the Fe_2O_3–V_2O_5–MoO_3 system in the solid state, do not remain at permanent equilibrium with each other but react to form mixtures containing two or three solid phases. Thus, in the subsolidus area of the system investigated, there were nine separate fields in which three solid phases coexisted at equilibrium, and two fields in which two solid phases remained at equilibrium.

The phase compositions of the separate fields and of the sections dividing these fields were confirmed by preparing 28 individual phases corresponding to the phase composition of the fields and to some of the sections dividing these fields. As mentioned above, the mixtures were heated for 72 h at temperatures slightly lower than those at which melting of the appropriate solidus planes or lines begins; following rapid cooling to ambient temperature, they were examined for their phase composition. X-ray powder diffraction showed that despite many hours of heating at temperatures close to the onset of melting, none of the compositions had changed. This implied that

TABLE 1

X-ray powder diffraction results for preparations at equilibrium from the basic and additional series

Number of preparation	Phases detected	Number of an area and lines dividing the fields
48	$FeVO_4$, $Fe_2V_4O_{13}$(s.s.)	I
18	$FeVO_4$, $Fe_2V_4O_{13}$(s.s.), $FeVMoO_7$	II
49	$FeVO_4$, $FeVMoO_7$, $Fe_4V_2Mo_3O_{20}$	III
5, 6, 7, 8, 13, 14,15,20, 25	$FeVO_4$, $Fe_4V_2Mo_3O_{20}$, Fe_2O_3	IV
26, 30	$Fe_4V_2Mo_3O_{20}$, Fe_2O_3, $Fe_2(MoO_4)_3$	V
50	$Fe_4V_2Mo_3O_{20}$, $Fe_2(MoO_4)_3$, $FeVMoO_7$	VI
31, 32, 35	$Fe_2(MoO_4)_3$, $FeVMoO_7$, $V_9Mo_6O_{40}$	VII
34, 36	$Fe_2(MoO_4)_3$, MoO_3, $V_9Mo_6O_{40}$	VIII
22, 27, 28, 37, 38	$V_9Mo_6O_{40}$, $FeVMoO_7$, V_2O_5(s.s.)	IX
11, 16, 17, 23, 42, 43	$FeVMoO_7$, V_2O_5(s.s.), $Fe_2V_4O_{13}$(s.s.)	X
1, 2, 3, 9, 10, 47	V_2O_5(s.s.), $Fe_2V_4O_{13}$(s.s.)	XI
33	$Fe_2(MoO_4)_3$, $Fe_4V_2Mo_3O_{20}$	V–VI
21	$Fe_4V_2Mo_3O_{20}$, Fe_2O_3	IV–V
29	$FeVMoO_7$, $Fe_4V_2Mo_3O_{20}$	III–VI
39, 40, 41	$FeVMoO_7$, V_2O_5(s.s.)	IX–X
44, 45, 46	V_2O_5(s.s.), $Fe_2V_4O_{13}$(s.s.)	X–XI
12, 24	$FeVO_4$, $FeVMoO_7$	II–III
19	$FeVO_4$, $Fe_4V_2Mo_3O_{20}$	III–IV
4	$FeVO_4$, $Fe_2V_4O_{13}$(s.s.)	I–II

the compositions of these selected mixtures corresponded to phases coexisting at equilibrium in particular fields and sections of the subsolidus area.

Figure 2 shows a projection of the Fe_2O_3–V_2O_5–MoO_3 solidus plane on the plane of the component concentration triangle constructed using the DTA curves and X-ray powder diffraction results for all the equilibrium preparations. Figure 2 also shows the melting temperatures of all the fields and the two-component sections on which the compositions of double eutectics (e) and the parameters of meritectic points (p) can be seen.

The lines dividing fields whose existence range is undisputed, have been marked with a full line, whereas the section whose route is thought probable in the light of the results obtained, has been marked with a dotted line. The uncertainty arises from the fact that the experimental results have not established unequivocably the existence range in the three-component system of a solid solution of MoO_3 and Fe_2O_3 in V_2O_5, nor the existence range of a field in which that solution would coexist with a solution of MoO_3 in $Fe_2V_4O_{13}$.

The phase equilibrium diagram of the subsolidus area (Fig. 2) is in agreement with the results obtained from previous studies of sections of the Fe_2O_3–V_2O_5–MoO_3 system [14–22].

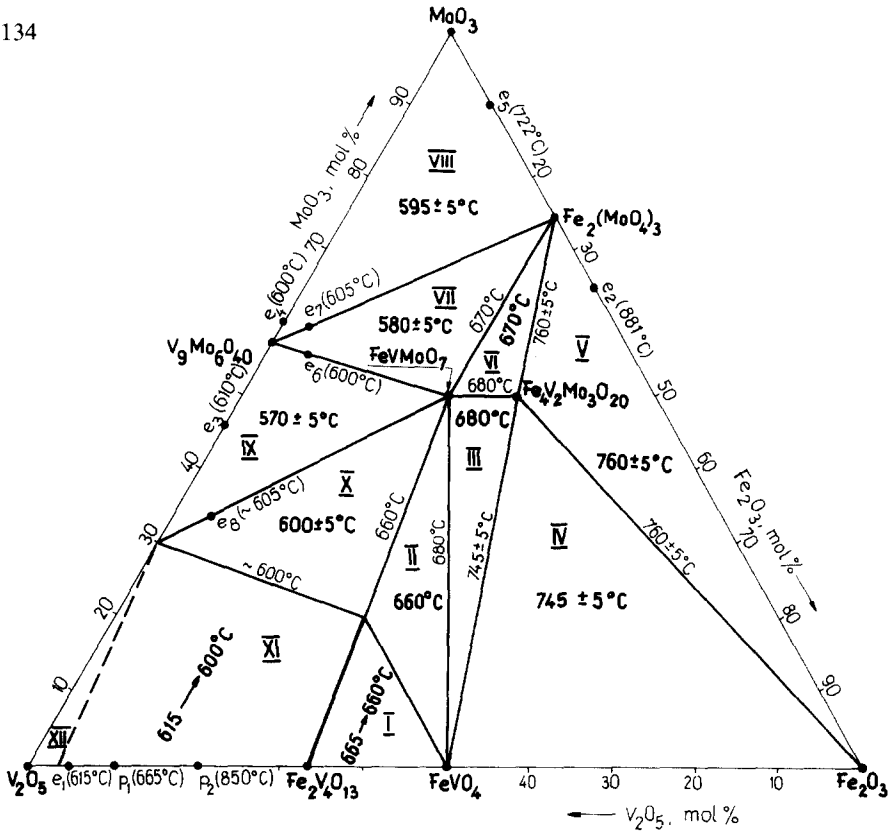

Fig. 2. Projection of the solidus plane of the Fe_2O_3–V_2O_5–MoO_3 system on the plane of the component concentration triangle.

The liquidus area of the Fe_2O_3–V_2O_5–MoO_3 system has been established by equations describing the temperature change in the area of the solid phase composition function. The equations were derived using an approximation of the experimental data with a quaternary polynomial for two independent variables, i.e. for the Fe_2O_3 and V_2O_5 concentrations expressed in molar percentages. The polynomial coefficients were calculated by the least-squares method. The source of the data were experimental results used for establishing the solidus area of the system, and results from the study of the pseudo-two-component systems making sections of a three-component system [14–22]. The literature data relevant to the two-component systems Fe_2O_3–V_2O_5, Fe_2O_3–MoO_3 and V_2O_5–MoO_3, were also used for this purpose. As there are insufficient experimental data for the $Fe_2V_4O_{13}$(s.s.) and Fe_2O_3 phases, the liquidus areas of the phases were determined graphically, as areas enclosed by points with known parameters. First, a run of isotherms on the liquidus area was determined. Then a run of lines of all the univariant equilibria was established, after finding the coordinates of the intersection points of the same isotherms of two adjoining liquidus areas. When an analytical determination of the run of the lines was impossible, a graphical extrapolation was employed for this purpose. The parameters of the invariant equilibrium points were also determined.

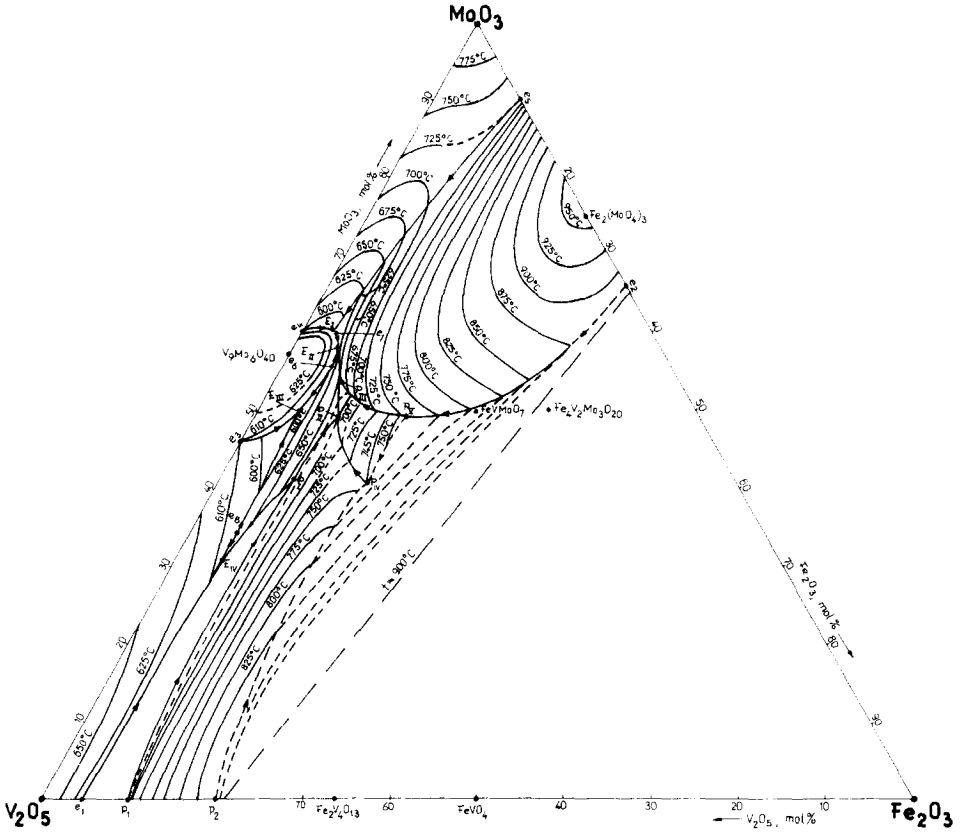

Fig. 3. Projection of the liquidus plane of the $Fe_2O_3-V_2O_5-MoO_3$ system on the plane of the component concentration triangle.

TABLE 2

Parameters of the invariant equilibrium points

Point	Solid phases coexisting with liquid at equilibrium	Temperature (°C)	Coordinates in the $Fe_2O_3-V_2O_5-MoO_3$ system (mol.%)		
			Fe_2O_3	V_2O_5	MoO_3
E_I	$Fe_2(MoO_4)_3$, MoO_3, $V_9Mo_6O_{40}$	595 ± 5	3.5	35.8	60.7
E_{II}	$Fe_2(MoO_4)_3$, $FeVMoO_7$, $V_9Mo_6O_{40}$	580 ± 5	5.0	37.5	57.5
E_{III}	$FeVMoO_7$, $V_9Mo_6O_{40}$, V_2O_5(s.s.)	570 ± 5	4.8	44.2	51.0
E_{IV}	$FeVMoO_7$, V_2O_5(s.s.), $Fe_2V_4O_{13}$(s.s.)	600 ± 5	5.0	64.0	31.0
P_I	$FeVO_4$, $Fe_2V_4O_{13}$(s.s.), $FeVMoO_7$	600	9.0	50.0	41.0
P_{II}	$FeVO_4$, $FeVMoO_7$, $Fe_4V_2Mo_3O_{20}$	680	10.0	41.0	49.0
P_{III}	$Fe_4V_2Mo_3O_{20}$, $FeVMoO_7$, $Fe_2(MoO_4)_3$	670	8.0	39.0	53.0
P_{IV}	$FeVO_4$, $Fe_4V_2Mo_3O_{20}$, Fe_2O_3	745 ± 5	16.5	43.0	40.5
P_V	$Fe_4V_2Mo_3O_{20}$, Fe_2O_3, $Fe_2(MoO_4)_3$	760	17.0	33.0	50.0

Figure 3 shows a projection of the liquidus area of the Fe_2O_3–V_2O_5–MoO_3 system on the plane of the component concentration triangle. The liquidus of this system is composed of areas of the following phases: MoO_3, $Fe_2(MoO_4)_3$, $V_9Mo_6O_{40}$, V_2O_5(s.s.), $Fe_2V_4O_{13}$(s.s.), $FeVO_4$, Fe_2O_3, $FeVMoO_7$ and $Fe_4V_2Mo_3O_{20}$.

The areas intersect to mark the invariant equilibrium lines along which melting of the following binary eutectics takes place: MoO_3–$Fe_2(MoO_4)_3$, MoO_3–$V_9Mo_6O_{40}$, $Fe_2(MoO_4)_3$–$V_9Mo_6O_{40}$, $V_9Mo_6O_{40}$–$FeVMoO_7$, $V_9Mo_6O_{40}$–V_2O_5(s.s.), $FeVMoO_7$–V_2O_5(s.s.), V_2O_5(s.s.)–$Fe_2V_4O_{13}$(s.s.) and Fe_2O_3–$Fe_2(MoO_4)_3$, as well as that of the pseudo-binary eutectics: $Fe_2(MoO_4)_3$–$FeVMoO_7$, $FeVMoO_7$–$Fe_2V_4O_{13}$(s.s.), $FeVO_4$–$FeVMoO_7$ and $FeVO_4$–$Fe_4V_2Mo_3O_{20}$.

In addition, the following binary meritectic reactions between the liquid and the solid phases, take place in the indicated temperature ranges:

$$\text{liquid} + FeVO_4(s) \underset{660\,^\circ C}{\overset{665\,^\circ C}{\rightleftarrows}} Fe_2V_4O_{13}(s.s.) \tag{3}$$

$$\text{liquid} + Fe_4V_2Mo_3O_{20}(s) \underset{670\,^\circ C}{\overset{680\,^\circ C}{\rightleftarrows}} FeVMoO_7(s) \tag{4}$$

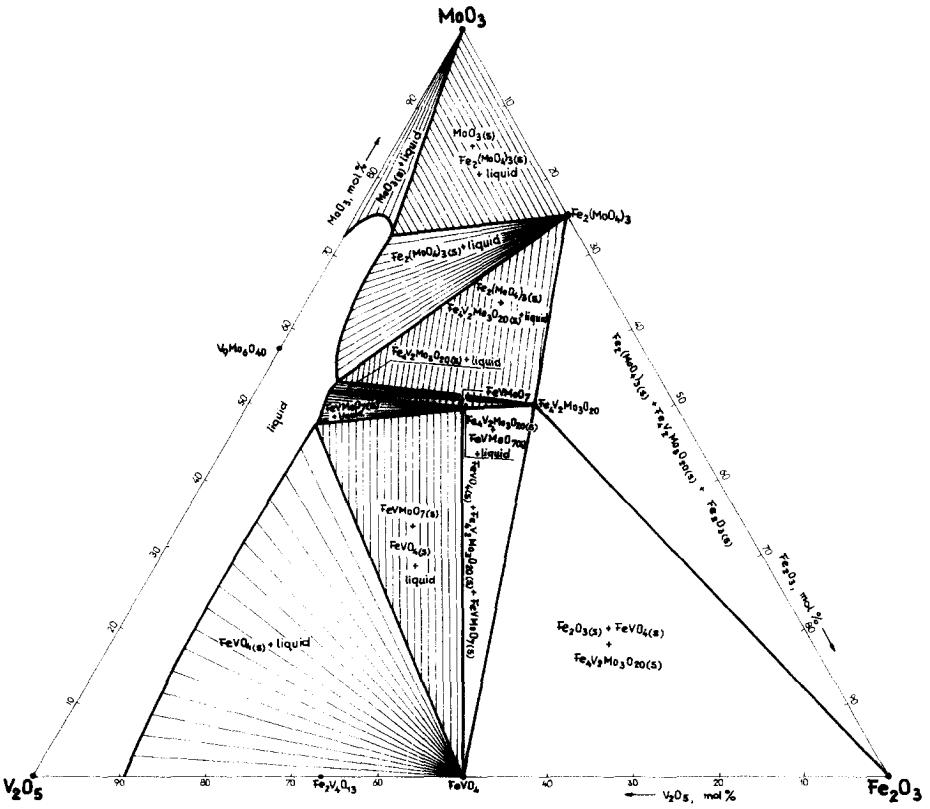

Fig. 4. Isothermal section of the ternary system Fe_2O_3–V_2O_5–MoO_3 at 675 °C.

$$\text{liquid} + Fe_2(MoO_4)_3(s) \overset{760\,^\circ C}{\underset{670\,^\circ C}{\rightleftarrows}} Fe_4V_2Mo_3O_{20}(s) \tag{5}$$

$$\text{liquid} + Fe_2O_3(s) \overset{760\,^\circ C}{\underset{745\,^\circ C}{\rightleftarrows}} Fe_4V_2Mo_3O_{20}(s) \tag{6}$$

$$\text{liquid} + Fe_2O_3(s) \overset{850\,^\circ C}{\underset{745\,^\circ C}{\rightleftarrows}} FeVO_4(s) \tag{7}$$

The eutectic and meritectic lines intersect at four ternary eutectic points (E) and at five points of quarternary meritectic equilibrium (P). The parameters of these points are presented in Table 2. The parameters of points E define the composition and melting temperature of the ternary eutectics, whereas the parameters of points P indicate the temperatures of the meritectic ternary reactions and the composition of the liquids involved in the latter reactions. The meritectic ternary reactions are

$$\text{liquid}_{P_I} + FeVO_4(s) \overset{660\,^\circ C}{\rightleftarrows} Fe_2V_4O_{13}(\text{s.s.}) + FeVMoO_7(s) \tag{8}$$

$$\text{liquid}_{P_{II}} + Fe_4V_2Mo_3O_{20}(s) \overset{680\,^\circ C}{\rightleftarrows} FeVMoO_7(s) + FeVO_4(s) \tag{9}$$

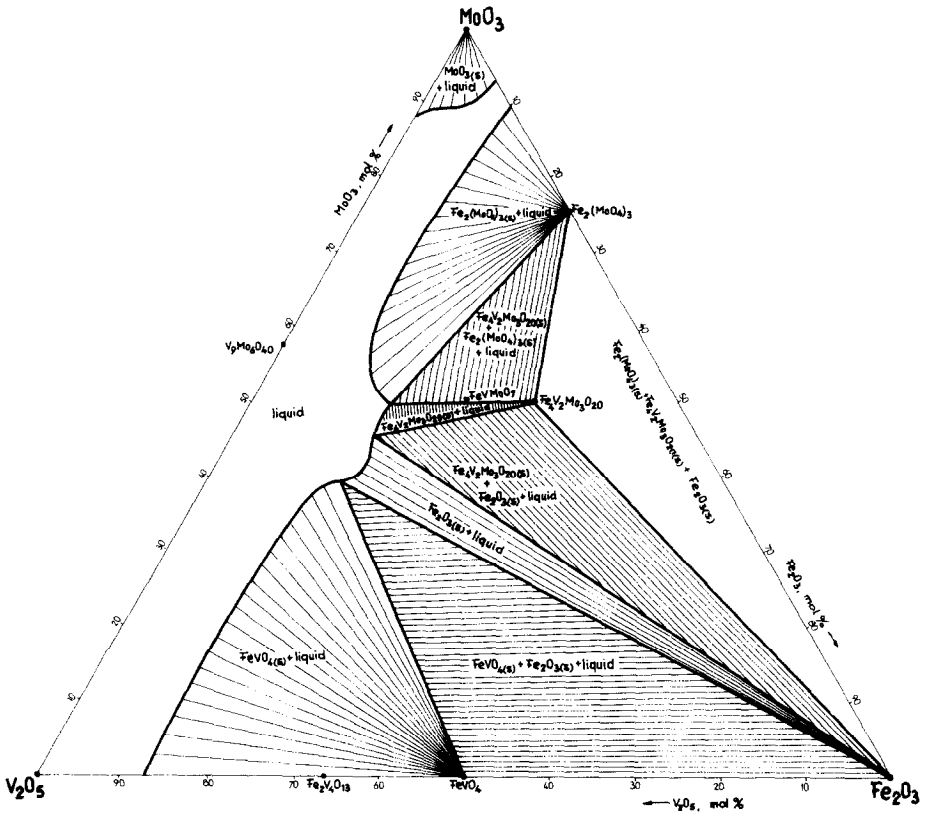

Fig. 5. Isothermal section of the ternary system Fe_2O_3–V_2O_5–MoO_3 at 750 °C.

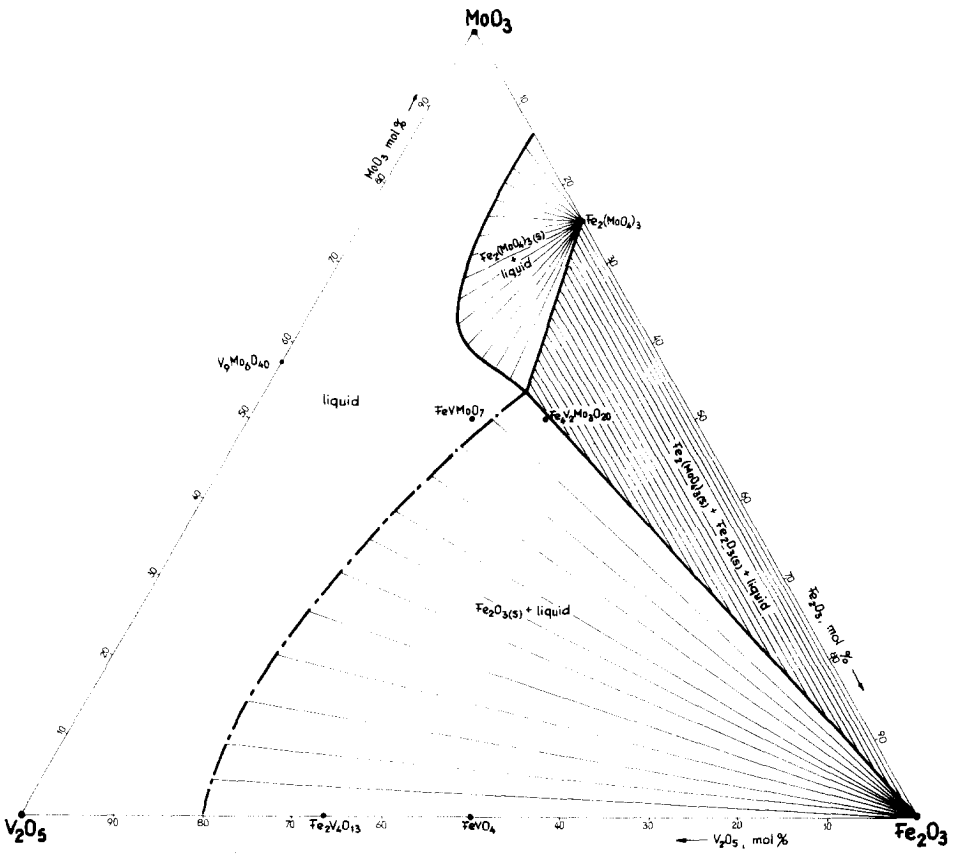

Fig. 6. Isothermal section of the ternary system Fe_2O_3–V_2O_5–MoO_3 at 850 °C.

$$\text{liquid}_{P_{III}} + Fe_4V_2Mo_3O_{20}(s) \overset{670\,^\circ C}{\rightleftarrows} Fe_2(MoO_4)_3(s) + FeVMoO_7(s) \quad (10)$$

$$\text{liquid}_{P_{IV}} + Fe_2O_3(s) \overset{745\,^\circ C}{\rightleftarrows} FeVO_4(s) + Fe_4V_2Mo_3O_{20}(s) \quad (11)$$

$$\text{liquid}_{P_V} + Fe_2O_3(s) + Fe_2(MoO_4)_3(s) \overset{760\,^\circ C}{\rightleftarrows} Fe_4V_2Mo_3O_{20}(s) \quad (12)$$

Figures 4, 5 and 6 show the phase equilibria established in the Fe_2O_3–V_2O_5–MoO_3 system at 675, 750 and 850 °C, respectively. The temperature of 675 °C was selected to show the field, $Fe_4V_2Mo_3O_{20}(s) + FeVMoO_7(s)$ + liquid, which exists in a very narrow temperature range, from 670 to 680 °C, and the field, $FeVMoO_7(s) + FeVO_4(s)$ + liquid, occurring between 660 and 680 °C. Figure 6 shows the phase equilibria established at 850 °C, the temperature at which a binary meritectic reaction takes place in the Fe_2O_3–V_2O_5 system: liquid + $Fe_2O_3(s) \rightleftarrows FeVO_4(s)$. In the three-component system, the reaction runs along the p_2P_{IV} line (Fig. 3) and ends at 745 °C at P_{IV}. On that cross-section, the field $Fe_2O_3(s) + FeVO_4(s)$ + liquid, narrows to the Fe_2O_3–p_2 line (Fig. 3).

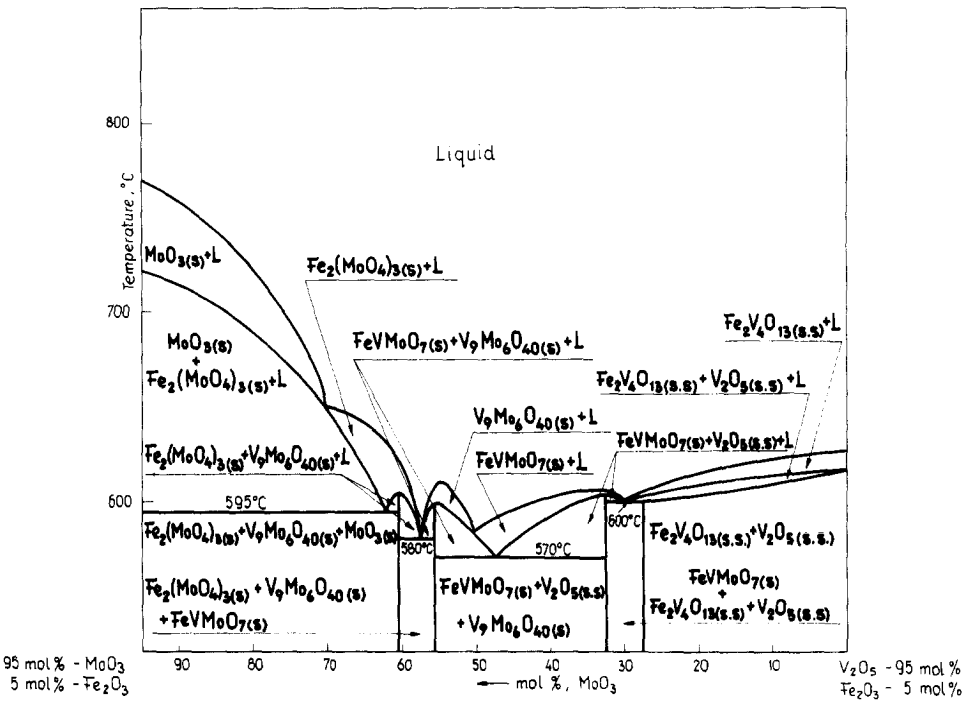

Fig. 7. Vertical section of the ternary system Fe_2O_3–V_2O_5–MoO_3 which represents constant concentration of Fe_2O_3 (5 mol.%).

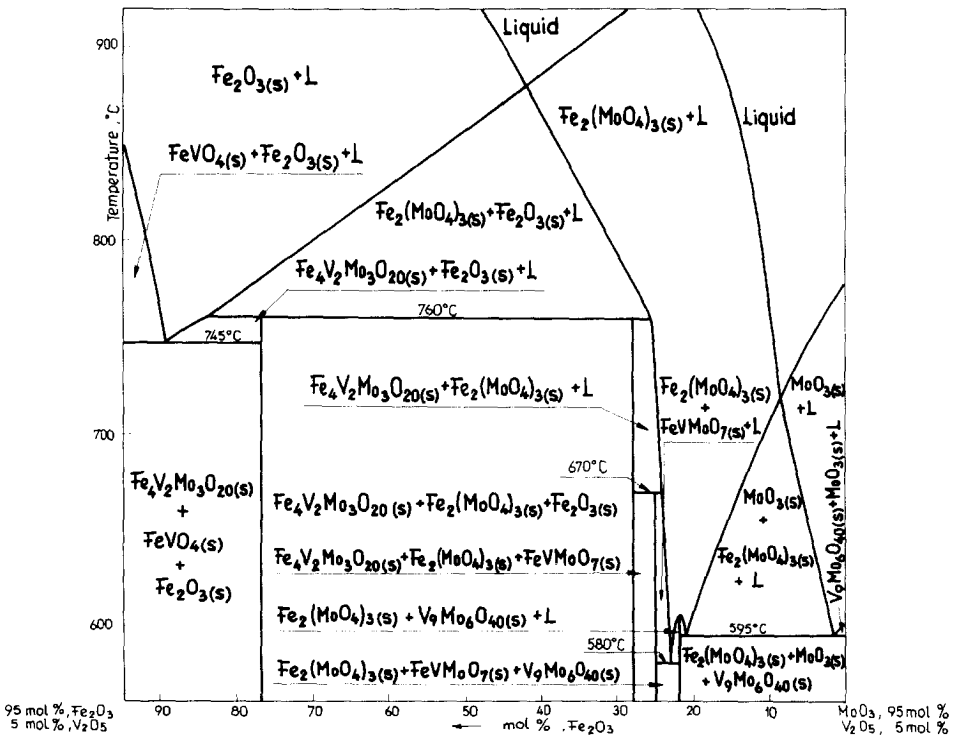

Fig. 8. Vertical section of the ternary system Fe_2O_3–V_2O_5–MoO_3 which represents constant concentration of V_2O_5 (5 mol.%).

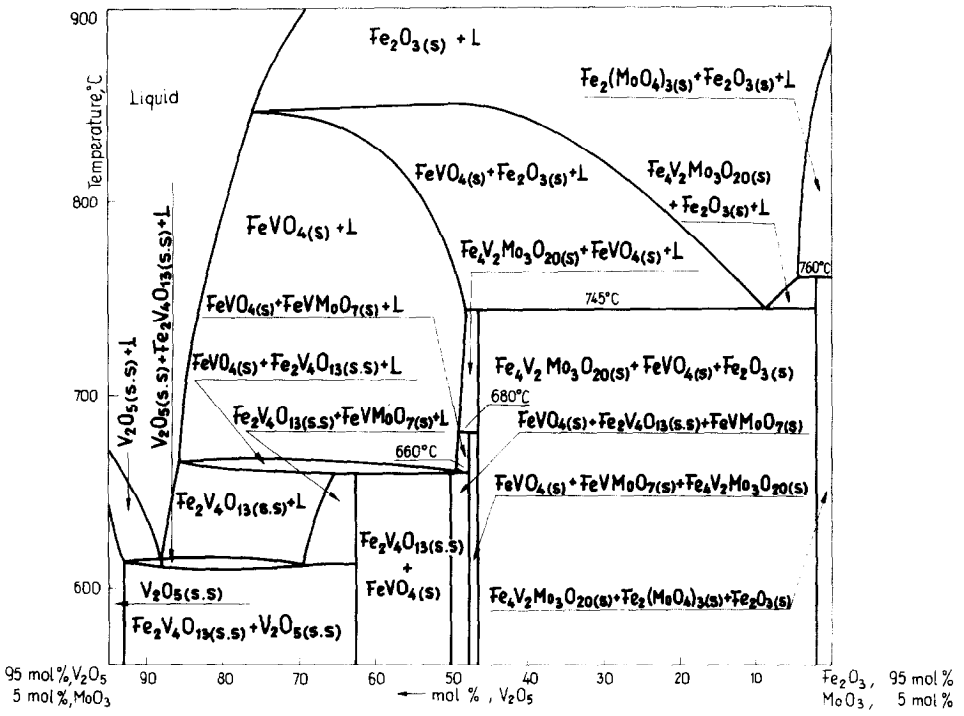

Fig. 9. Vertical section of the ternary system Fe_2O_3–V_2O_5–MoO_3 which represents constant concentration of MoO_3 (5 mol.%).

The liquid fields have not been delineated in the diagrams. The two-phase fields (one solid phase and one liquid phase) have been marked with lines radiating from a given phase, whereas phases in which two solid phases + a liquid exist, have been marked with parallel lines.

Areas that have not melted are described by solid phases coexisting at equilibrium. They too have not been delineated.

The investigations were used to construct polythermal cross-sections in which the contents of one of the components was constant at around 5 mol.%. These sections are shown in Figs. 7, 8 and 9.

REFERENCES

1 A.M. El-Awad, E.A. Hassan, A.A. Said and K.M. Abd El-Salaam, Monatsh. Chem., 120 (1989) 199.
2 G. Allessandrini, L. Cairati, P. Forzatti, P. Villa and F. Trifiro, J. Less-Common Met., 54 (1977) 373.
3 J.A. Dorfman, Katalizatory i mekhanizmy gidrirovaniya i okisleniya, Alma-Ata, 1984, izd. Nauka Kazakhskoy SSR.
4 J. Chrząszcz, B. Draniak, J. Obłój, W. Ormaniec, W. Wal, A. Jakubowicz and E. Wizner, Przem. Chem., 57 (1978) 173.
5 N. Van Truong, P. Tittarelli and P. Villa, in H.F. Barry and P.C.H. Mitchell (Eds.), Proc. III Int. Conf. Chem. Uses Molybdenum, Ann Arbor, Michigan, (1979) 161.

6 F. Trifiro and I. Pasquon, J. Catal., 12 (1968) 412.
7 W. Jäger, A. Rahmel and K. Becker, Arch. Eisenhüttenwes., 30 (1959) 435.
8 H.Y. Chen, Mater. Res. Bull., 14 (1979) 1583.
9 J. Walczak, J. Ziółkowski, M. Kurzawa, J. Osten-Sacken and M. Łysio, Pol. J. Chem., 59 (1985) 255.
10 B. Robertson and K. Kostiner, J. Solid State Chem., 4 (1972) 29.
11 A. Bielański, K. Dyrek, J. Poźniczek and E. Wenda, Bull. Acad. Polon. Sci., Ser. Sci. Chim., 19 (1971) 507.
12 R.H. Jarman and A.K. Cheetham, Mater. Res. Bull., 17 (1982) 1011.
13 Z.C. Kang, Q.X. Bao and C. Boulesteix, J. Solid State Chem., 83 (1989) 255.
14 J. Walczak, J. Ziółkowski, M. Kurzawa and L. Trześniowska, Pol. J. Chem., 59 (1985) 713.
15 J. Walczak, M. Kurzawa and E. Filipek, J. Therm. Anal., 31 (1986) 271.
16 J. Walczak, M. Kurzawa, J. Frąckowiak and T. Panek, J. Mater. Sci. Lett., 5 (1986) 1224.
17 J. Walczak and M. Kurzawa, J. Therm. Anal., 31 (1986) 531.
18 J. Walczak and M. Kurzawa, Thermochim. Acta, 127 (1988) 363.
19 J. Walczak, M. Kurzawa and P. Tabero, Thermochim. Acta, 118 (1987) 1.
20 J. Walczak and M. Kurzawa, J. Therm. Anal., 34 (1988) 679.
21 J. Walczak, M. Kurzawa and P. Tabero, J. Therm. Anal., 33 (1988) 969.
22 J. Walczak, M. Kurzawa and E. Filipek, Thermochim. Acta, 117 (1987) 9.
23 M. Kurzawa, Proc. 8th Int. Conf. Therm. Anal., ICTA'85, Bratislava, August 19–23, 1985; Thermochim. Acta, 92 (1985) 563.
24 M. Kurzawa, Abstracts of Poster Comm. 31st Int. Congress of Pure and Applied Chem., IUPAC'87, Sofia, July 13–18, 1987, Vol. 1, p. 5.172.
25 R.H. Jarman, P.G. Dickens and A.J. Jacobson, Mater. Res. Bull., 17 (1982) 325.
26 Joint Committee of Powder Diffraction File: 19-813, 20-526, 20-1377, 24-541, 25-418, 31-642, 33-661, 33-664, 34-527, 35-183.